

Relaxor Ferroelectric-Like Behavior in Barium Titanate-Doped Glass via Formation of Polar Clusters

M. M. El-Desoky¹ · A. E. Harby¹ · Ahmed E. Hannora² ·
M. S. Al-Assiri³

Received: 17 February 2017 / Published online: 13 April 2017
© Springer Science+Business Media New York 2017

Abstract Glass lead free sample of composition $10\text{BaTiO}_3\text{--}60\text{V}_2\text{O}_5\text{--}30\text{B}_2\text{O}_3$ in mol% was prepared by conventional melt quenching technique. The as-prepared sample shows relaxor ferroelectric-like behavior which is a novel phenomenon in the field of glass science. XRD and DSC were used to emphasize the glassy nature of the present sample. Diffraction spots from clusters are clearly observed using HRTEM, which is presumably from polar clusters (PCs). The sample shows a broad and diffuse peak in the temperature dependence of dielectric permittivity ϵ' (T) and tangent loss, the temperature of which increases with increasing measuring frequency, denoting the typical relaxor behavior. The existence of distorted BaTiO_3 PCs embedded in the glass matrix is responsible for the appearance of this behavior. The present glass sample shows energy storage density of about 0.11 J/cm^3 at room temperature and 0.44 J/cm^3 at $120\text{ }^\circ\text{C}$, which is reasonably good for bulk polar material. The results obtained in this work could lay the basis for the development of lead free materials to meet the energy storage and Eco-friendly applications.

Keywords Glasses · Polar clusters · Relaxor ferroelectrics · Energy storage density

✉ M. M. El-Desoky
mmdesoky@suezuniv.edu.eg

¹ Department of Physics, Faculty of Science, Suez University, Suez, Egypt

² Department of Science and Mathematical Engineering, Faculty of Petroleum and Mining Engineering, Suez University, Suez 43721, Egypt

³ Physics Department, College of Science and Arts, Najran University, Najran, Kingdom of Saudi Arabia

Introduction

Since the discovery of relaxor ferroelectrics in the 1950s, these new materials have shown unique properties, many of which are not yet understood. In the last few years scientists have developed this field by introducing new relaxor ferroelectric materials [1, 2]. Ceramics, solid solutions of complex perovskite and polymers are common examples of such materials accompanied by amazing dielectric and piezoelectric properties. To date, any material for which the real part of the dielectric constant shows a broad peak at a temperature T_m that depends strongly on the measuring frequency, f , is classified as a relaxor [3]. This behavior is associated with the relaxation of special type of dipoles arising from compositional inhomogeneity. Due to the compositional disorder, long-range polar ordering is prevented, and instead, polar nanoregions (PNRs) and nano-domains appear in relaxor ferroelectrics [4, 5]. Generally, relaxor ferroelectrics exhibits diffusive and frequency dependent dielectric anomalous their specific properties are associated with the presence of PNRs [6].

Glass of relaxor ferroelectric properties is considered as an anomalous phenomenon in the field of glass science. Glasses are amorphous solids exhibit transition temperature T_g which is obtained after solidification of a supercooled liquid. Glasses are characterized by the existence of short and intermediate range order in the atomic scale. Their structural network is divided into nanometer regions (clusters). The crystal ordered region is estimated to cover several tens to a hundred of atoms and to have a diameter of $\sim(1.0\text{--}1.5)$ nm [7]. Such a very small size the substance remains X-ray amorphous. It is supposed that nano-clusters in glasses arise at the transition from the low-viscosity state of the liquid (melt) to the high-viscosity state. The temperature of such transition depends on the complexity of the architecture of molecules that compose the liquid [7]. The formation process of PNRs in relaxors is similar to that of glass formation. It was found that the similarity of the structure of glasses and relaxors at the nanoscale is related to the process of their growth from the high-temperature phase of the original products [7–10].

Glasses in general show linear dielectric response, small polarization and low permittivity besides high breakdown strength. However, relaxor ferroelectrics via formation of PCs embedded in glass matrix have an enormous potential in designing new polar dielectrics for energy storage applications due to high dielectric constant and high energy storage capacity.

In this work, we discuss a novel phenomenon, the existence of PCs and the appearance of relaxor ferroelectric behavior in $10\text{BaTiO}_3\text{--}60\text{V}_2\text{O}_5\text{--}30\text{B}_2\text{O}_3$ glass sample. The glass was characterized using X-ray diffraction (XRD), differential scanning calorimetry (DSC), High resolution transmission electron microscope (HRTEM), Raman scattering, dielectric spectroscopy as well as measuring ferroelectric hysteresis loops. The relaxor ferroelectric and nanostructure properties of this lead free glass sample are discussed in the situation of its capability to Eco-friendly and energy storage applications.

Synthesis of Glass and Materials Characterization

Glass lead free sample of composition $10\text{BaTiO}_3\text{-}60\text{V}_2\text{O}_5\text{-}30\text{B}_2\text{O}_3$ in mol % was prepared by conventional melt quenching technique following the same procedures illustrated in Ref. [11]. To confirm the glass nature of the sample a room temperature X-ray (PANalytical Empyrean diffractometer) diffraction pattern was taken using $\text{Cu K}\alpha$ radiation over a wide range of Bragg angle 2θ ($10\text{-}100^\circ$) and a scan rate of $0.02^\circ/\text{s}$. The heat flow of the sample was measured by differential scanning calorimeter (Shimatrou DSC 50 instrument). DSC data collected up to (500°C) employing a heating rate of $10^\circ\text{C}/\text{min}$. High resolution transmission electron microscope (HRTEM) model (JEOL 2100) was used to verify the existence of nano-clusters embedded in the glass matrix. Room temperature Raman studies were carried out using LabRAM-HR (Horiba Jobin-Yvon) in the spectral range from 1000 to 50 cm^{-1} . As excitation source we used the 632.8 nm line of a He-Ne Laser. Dielectric measurements were carried out at various frequencies as a function of temperature using LCR meter at oscillating amplitude of 1 V . The polarization– electric field (P–E) hysteresis loops of the sample were measured using a Sawyer–Tower circuit.

Results and Discussion

DSC thermogram for the glass sample is shown in Fig. 1a. The present glass sample exhibits endothermic minimum which is corresponding to the glass transition temperature T_g (320°C) confirming the glass nature of the sample. At this

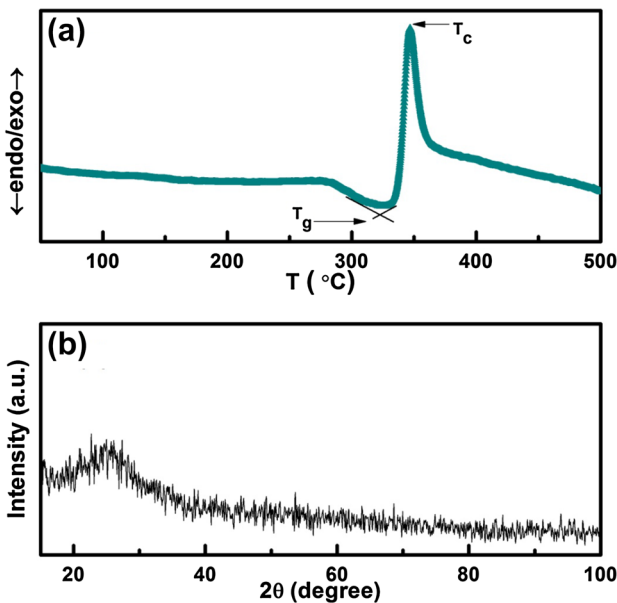


Fig. 1 a The DCS pattern and b XRD of $10\text{BaTiO}_3\text{-}60\text{V}_2\text{O}_5\text{-}30\text{B}_2\text{O}_3$ glass

temperature the atoms begin to arrange themselves in precursory structure elements preceding the nucleation. This sample also exhibits an exothermic peak T_c (347 °C) corresponding to crystallization temperature. The appearance of a single peak due to the glass transition temperature in DSC pattern of glass sample denotes the existence of high homogeneity in the present glass [12]. XRD pattern of the prepared sample is shown in Fig. 1b. From this figure, it is observed that a homogenous glass is formed. This glassy behavior shows a broad hump at $2\theta \approx 25^\circ$. The overall feature of this XRD pattern confirms the amorphous nature of the present glass [13].

High resolution transmission electron microscope (HRTEM) was used to verify the existence of nano-clusters embedded in the glass matrix. HRTEM along with the selective area electron diffraction pattern (SAED) of the as-quenched $10\text{BaTiO}_3\text{-}60\text{V}_2\text{O}_5\text{-}30\text{B}_2\text{O}_3$ glass is shown in Fig. 2. Figure 2 shows the existence of V_2O_5 nano-clusters and distorted BaTiO_3 polar clusters (PCs) in the glass matrix; which may responsible for large dielectric dispersion and relaxor ferroelectric. The values of d spacing calculated from HRTEM are 0.234 and 0.285 nm which is very close to d spacing values of the planes 111 and 101 of BaTiO_3 , respectively. However, the other d spacing value is 0.339 nm represent V_2O_5 nano-clusters for 101 planes. It is found from HRTEM observations that the crystalline phases inside the glass matrix have some disordering. The crystal defects appears as; discontinuity, and a mixture of long and short range ordering as well as the presence of a large number of twin boundaries. These observations support the relaxor character of the sample. The SAED pattern that is shown in the inset of Fig. 2 confirms the amorphous state. However, a diffraction spots from clusters is clearly observed, which is presumably from PCs.

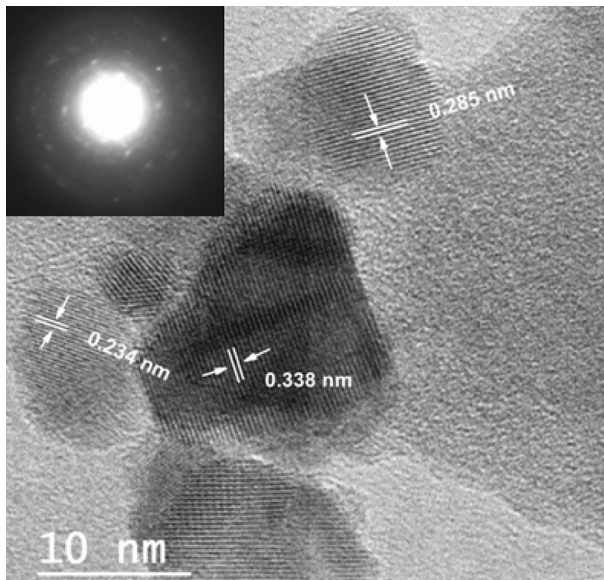


Fig. 2 HRTEM of $10\text{BaTiO}_3\text{-}60\text{V}_2\text{O}_5\text{-}30\text{B}_2\text{O}_3$ glass. The *inset* represents SAED of the sample

Room temperature Raman scattering measurement has been carried out on $10\text{BaTiO}_3\text{-}60\text{V}_2\text{O}_5\text{-}30\text{B}_2\text{O}_3$ glass (Fig. 3). The following peaks are present in this figure: 92, 157, 254, 404, 500, 690 and 920 cm^{-1} . The low frequency Raman spectra shows a peak (Boson peak) at 92 cm^{-1} . However, it is not completed due to the experimental limitations of the Raman spectrometer. This Boson peak is associated with the existence of intermediate range order in glass. The intermediate range order denotes that the arrangements of structural units in a glass are not completely random but have some correlations on a nanometer scale varying slightly between different glasses [14]. According to Freire and Katiyar [15], the low frequency peak observed at 157 cm^{-1} corresponds to a motion of the barium ions against the BO_6 octahedra. The peak around at 254 cm^{-1} represents the oxygen ion vibration with different positions inside the clusters. Glasses with high V_2O_5 content shows peak around 404 cm^{-1} from crystalline V_2O_5 nano-clusters, this peak overlapped with the peak observed at 500 cm^{-1} , which is due to O–Ti–O symmetric stretching vibrations [16]. Polar $[\text{VO}_6]$ and especially $[\text{TiO}_6]$ clusters are responsible for the peak observed at around 690 cm^{-1} [17]. The peak observed at the high frequency range 920 cm^{-1} is attributed to the stretching vibrations of B–O bonds in orthoborate formed by pyramidal BO_3 unit.

Figure 4a and b shows the real part of the dielectric constant (ϵ') and tangent loss ($\tan\delta$) data as a function of temperature at increasing frequencies from 0.5 to 100 kHz. High and diffusive dielectric constant was shown in Fig. 4a and b, shifting of the dielectric maximum temperature (T_m) towards higher temperature with increasing frequency which represents the relaxor behavior. The existence of distorted BaTiO_3 PCs embedded in the glass matrix is responsible for the appearance of this behavior. The degree of relaxation behavior, obtained by $\Delta T_{\text{relaxor}} = T_m(100\text{kHz}) - T_m(0.5\text{kHz})$ is found to be 56 K [18, 19]. The relaxation of relaxor ferroelectrics is considered as a thermally activated process which is commonly believed to be similar to a spin or dipole glass that the dynamics are only

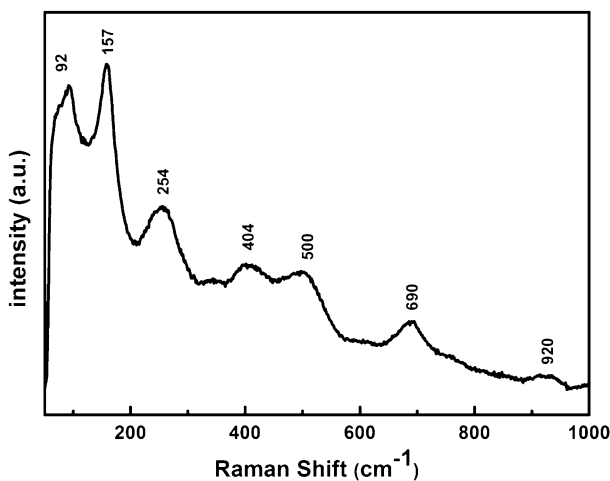


Fig. 3 Raman spectroscopy of $10\text{BaTiO}_3\text{-}60\text{V}_2\text{O}_5\text{-}30\text{B}_2\text{O}_3$ glass

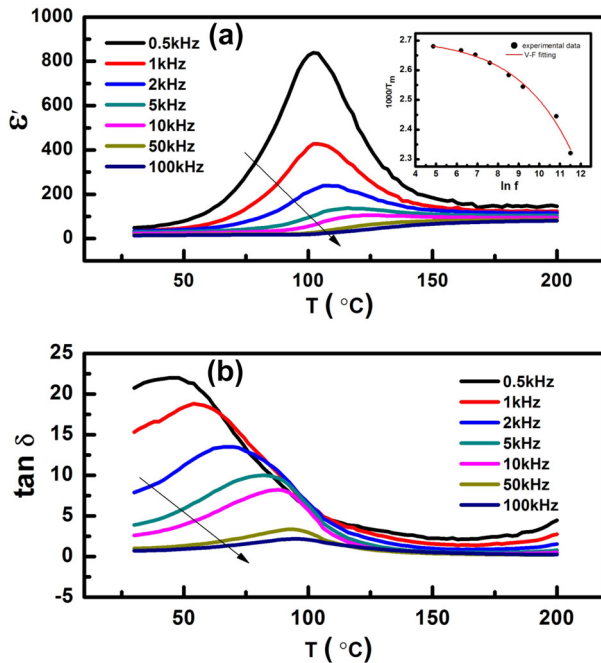


Fig. 4 Temperatures and frequency dependent (a) dielectric constant (b) loss tangent of $10\text{BaTiO}_3\text{-}60\text{V}_2\text{O}_5\text{-}30\text{B}_2\text{O}_3$ glass the *inset* of (a) shows the non-linear Vogel-Fulcher fit of the dielectric data

activated above a finite freezing temperature [20, 21]. The T_m values of the dielectric spectra were fitted using a nonlinear Vogel-Fulcher (VF) relation as shown in the inset of Fig. 4a [22, 23].

$$f = f_0 \exp\left(\frac{-E_a}{k_B(T_m - T_f)}\right)$$

where f is the experimental frequency, f_0 the pre-exponential factor, E_a the activation energy, k_B the Boltzmann constant; and T_f , the freezing temperature (i.e. the temperature below which the relaxation time becomes infinite). The fitted parameters $E_a = 0.03$ eV, $f_0 = 3 \times 10^6$ Hz, and $T_f = 333$ K.

Similar frequency dependent was observed in the loss tangent as shown in Fig. 4b. It follows the same behavior of frequency response as that of the dielectric constant. Obviously, the dielectric loss data and their dispersion with frequency and temperature provide additional confirmation of the relaxation behavior than the dielectric constant values alone. Also, the tangent loss data exhibits high dielectric loss that release to the high conductivity already known for such vanadate glasses [11].

The identification of the nature of such dielectric response still remains open and requires more theoretical and experimental information, which can be very interesting to contribute to the investigation of this field especially by introducing

a new system. However, the mechanism of this behavior is still under intensive investigation, it is supposed to be related to the relaxation of dipoles arising from chemical order/disorder and short range polar order [24]. Due to the compositional disorder, long range polar ordering is prevented and PCs form instead of macroscopic domains which occur in normal ferroelectrics. At high enough temperatures it is assumed that the dipolar moments of PCs change in direction due to thermal motion. Upon cooling, the PCs increase in number and size, causing the permittivity to increase, while simultaneously, the PCs dynamics slows down, until at some point, the moments can no longer keep up with the oscillating measuring voltage, resulting in a maximum of dielectric permittivity occurring at different T_m for different frequencies [24].

The energy storage behavior of the present glass sample was investigated by the P–E hysteresis loop. Figure 5 shows the P–E loops of the sample measured at room temperature and 50 Hz at different applied electric fields. The loop reveals a remnant polarization (P_R) of about $2.53 \mu\text{C}/\text{cm}^2$ and coercive field (E_C) of about 198 kV/cm. The energy storage density (J) is obtained by integrating the area between the polarization axis and the discharge curve (yellow shaded region) of the loop according to the equation [25]:

$$J = \int E dP$$

where E is the applied electric field and P is polarization. The sample shows energy density of about $0.11 \text{ J}/\text{cm}^3$ at 600 kV/cm, the inset of Fig. 5 shows the charge and discharge energy densities:

$$U_d = \text{area II}$$

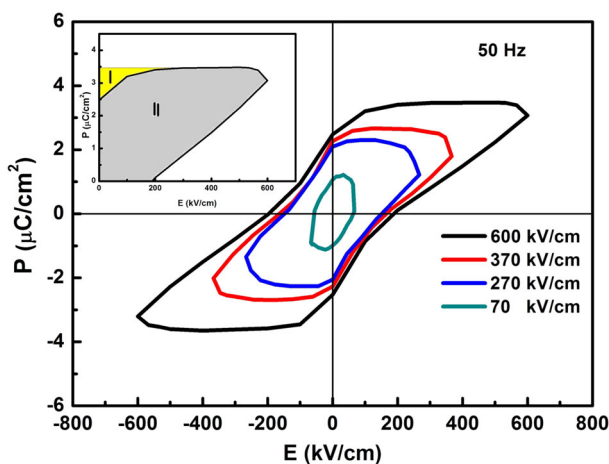


Fig. 5 The P–E loop of the glass sample at different electric fields. The *inset* shows the charge–discharge cycle of $10\text{BaTiO}_3\text{--}60\text{V}_2\text{O}_5\text{--}30\text{B}_2\text{O}_3$ glass

$$U_c = \text{area I} + \text{II}$$

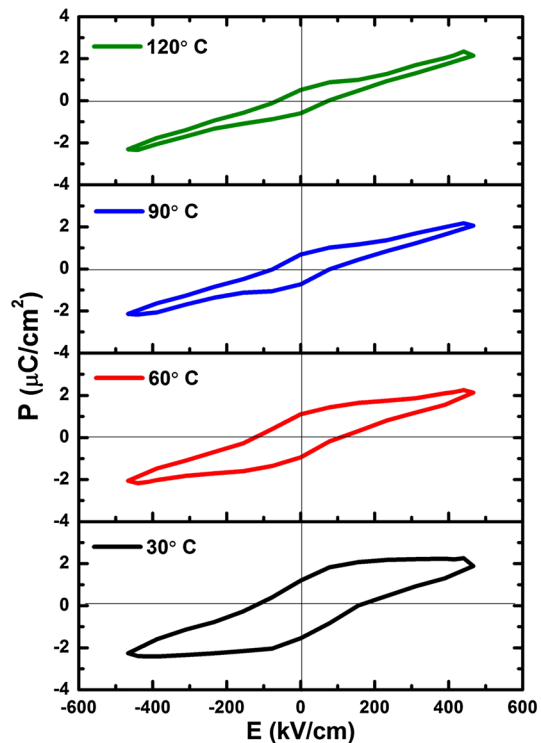
The charge–discharge efficiency (η) of the capacitors was calculated using the relation:

$$\eta = \frac{U_d}{U_c} \times 100\%$$

The efficiency of the glass sample at 600 kV/cm varied from 13.5 to 71% at room temperature and 120 °C, respectively.

Figure 6 shows the temperature dependent P–E hysteresis loops for the present glass sample. At room temperature the glass exhibits typical ferroelectric-like shaped loop with large P_R and E_C . A relaxor, on the other hand, displays a so-called slim loop. For sufficiently high electric fields the nanodomains of the relaxor can be oriented with the field leading to large polarization; however, on removing the field most of these domains iterate their random orientations resulting in a small P_R [26]. We can assume that, the presence of large P_R in this work is attributed to the complexity in the structure of the glass sample. With further increasing temperature the E_C and P_R values decrease dramatically and the loop becomes slimmer suggesting a high potential to store energy up to 0.44 J/cm³ at 120 °C. It is interesting to note that the maximum polarization does not change with the increase

Fig. 6 The P–E loops of 10BaTiO₃–60V₂O₅–30B₂O₃ glass as a function of temperature



in temperature. These features suggest that lead-free glass sample can be considered as a promising candidate for large variety of applications [27, 28].

Conclusion

We have found for the first time a relaxor ferroelectric-like behavior in 10BaTiO₃–60V₂O₅–30B₂O₃ glass sample. The present glass sample shows amazing properties, the existence of distorted BaTiO₃ PCs inside the glass matrix which is responsible for the appearance of the relaxor ferroelectric-like behavior. Also, P–E hysteresis loop for the present lead free glass sample at room temperature exhibits ferroelectric-like shape loop with large values of E_C and P_R , possessing an energy density of about 0.11 J/cm³ at room temperature and 0.44 J/cm³ at 120 °C, which can be considered as a promising candidate for energy storage and Eco-friendly applications especially at high temperatures.

Acknowledgements We thank, Dr. Stanislava MILOVSKÁ, Earth Science Institute of the Slovak Academy of Sciences, Slovakia for measure the Raman Spectrograph sample.

References

1. G. Xu, W. Wen, C. Stock, and P. M. Gehring (2008). *Nat. Mater.* **7**, 562–566.
2. M. E. Manley, J. W. Lynn, D. L. Abernathy, E. D. Specht, O. Delaire, A. R. Bishop, R. Sahul, and J. D. Budai (2014). *Nat. Commun.* **5**, 3683.
3. D. Phelan, C. Stock, J. A. Rodriguez-Rivera, S. Chi, J. Leão, X. Long, Y. Xie, A. A. Bokov, Z. G. Ye, P. Ganesh, and P. M. Gehring (2014). *Proc. Natl. Acad. Sci.* **111**, 1754.
4. A. A. Bokov and Z. G. J. Ye (2006). *Mat. Sci.* **41**, 31–52.
5. Z. G. Ye (1998). *Key. Eng. Mat.* **155–156**, 81–122.
6. L. E. Cross (1987). *Ferroelectrics* **76**, 267.
7. V. K. Malinovsky (2014). *Optoelectron. Instrum. Data Process.* **50**, 556–565.
8. G. A. Smolenskii and V. A. Isupov (1954). *Dokl Acad Nauk SSSR.* **97**, 653.
9. D. Fu, H. Taniguchi, M. Itoh, S. Y. Koshihara, N. Yamamoto, and S. Mori (2009). *Phys. Rev. Lett.* **24**, (103), 207601.
10. Y. Imry and S. K. Ma (1975). *Phys. Rev. Lett.* **35**, 1399.
11. A. E. Harby, A. E. Hannora, M. S. Al-Assiri, and M. M. El-Desoky (2016). *J. Mater. Sci: Mater. Electron.* **27**, 8446–8454.
12. A. A. Bahgat, M. G. Moustafa, and E. E. Shaisha (2013). *J. Mater. Sci. Technol.* **29**, 1166–1176.
13. M. M. El-Desoky (2010). *Mater. Chem. Phys.* **119**, 389–394.
14. J. Schroeder, W. Wu, J. L. Apkarian, M. Lee, L. G. Hwa, and C. T. Moynihan (2004). *J. Non-Cryst. Solids* **349**, 88–97.
15. J. D. Freire and R. S. Katiyar (1988). *Phys. Rev. B.* **37**, 2074.
16. J. C. Sczancoski, L. S. Cavalcante, T. Badapanda, S. K. Rout, S. Panigrahi, V. R. Mastelaro, J. A. Varela, M. S. Li, and E. Longo (2010). *Solid State Sci.* **12**, 1160–1167.
17. A. Dixit, S. B. Majumder, P. S. Dobal, R. S. Katiyar, and A. S. Bhalla (2004). *Thin Solid Films* **447**, 284–288.
18. T. Strathdee, L. Luisman, A. Feteira, and K. Reichmann (2011). *J. Am. Ceram. Soc.* **94**, 2292–2295.
19. X. Huang, H. Hao, S. Zhang, H. Liu, W. Zhang, Q. Xu, and M. Cao (2014). *J. Am. Ceram. Soc.* **97**, 1797–1801.
20. H. Y. Guo, C. Lei, and Z. G. Ye (2008). *Phys. Rev. Lett.* **92**, 2901.
21. S. S. N. Bharadwaja, J. R. Kim, H. Ogihara, L. E. Cross, S. Trolier-McKinstry, and C. A. Randall (2011). *Phys. Rev. B.* **83**, 024106.
22. H. Vogel (1921). *Phys. Z.* **22**, 645. CASI Web of Science® Times Cited (1932).

23. I. Rivera, A. Kumar, N. Ortega, R. S. Katiyar, and S. Lushnikov (2009). *Solid State Commun.* **149**, 172–176.
24. H. N. Tailor, A. A. Bokov, and Z. G. Ye (2011). *Curr. Appl. Phys.* **11**, S175–S179.
25. N. Ortega, A. Kumar, J. F. Scott, D. B. Chrissey, M. Tomazawa, S. Kumari, D. G. B. Diestra, and R. S. Katiyar (2012). *J. Phy.: Condens. Matter* **24**, (44), 445901.
26. G. A. Samara (2003). *J. Condens. Mater.* **15**, R367.
27. H. Borkar, V. N. Singh, B. P. Singh, M. Tomar, V. Gupta, and A. Kumar (2014). *RSC Adv.* **4**, 22840.
28. M. Zannen, A. Lahmar, H. Khemakhem, and M. El Marssi (2016). *Solid State Commun.* **245**, 1–4.